THE JOURNAL OF BIOLOGICAL CHEMISTRY VOL. 287, NO. 27, pp. 22822–22826, June 29, 2012

Solid-state NMR Reveals a Close Structural Relationship between Amyloid-β Protofibrils and Oligomers*[S]

Received for publication, March 30, 2012, and in revised form, May 9, 2012 Published, JBC Papers in Press, May 15, 2012, DOI 10.1074/jbc.M112.367474

Holger A. Scheidt[‡], **Isabel Morgado**[§], **and Daniel Huster**[‡1]

From the [‡]*Institute of Medical Physics and Biophysics, University of Leipzig, D-04107 Leipzig and the* [§]*Institute of Biochemistry/Biotechnology, Martin-Luther-Universität Halle-Wittenberg, D-06120 Halle, Germany*

Background: Little tertiary structure information is available for the toxic intermediates in the amyloid-β (Aβ) fibrillation process.
Results: Aβ protofibrils show tertiary contacts between Glu-22 and Ile-31, which are not present in mature fibrils.
Conclusion: Aβ protofibrils share tertiary structure features with oligomers but not with mature fibrils.
Significance: Aβ protofibrils must undergo a major structural reorientation in the development of mature Aβ fibrils.

We have studied tertiary contacts in protofibrils and mature fibrils of amyloid-β (Aβ) peptides using solid-state NMR spectroscopy. Although intraresidue contacts between Glu-22 and Ile-31 were found in Aβ protofibrils, these contacts were completely absent in mature Aβ fibrils. This is consistent with the current models of mature Aβ fibrils. As these intramolecular contacts have also been reported in Aβ oligomers, our measurements suggest that Aβ protofibrils are structurally more closely related to oligomers than to mature fibrils. This suggests that some structural alterations have to take place on the pathway from Aβ oligomers/protofibrils to mature fibrils, in agreement with a model that suggests a conversion of intramolecular hydrogen-bonded structures of Aβ oligomers to the intermolecular stabilized mature fibrils (Hoyer, W., Grönwall, C., Jonsson, A., Ståhl, S., and Härd, T. (2008) *Proc. Natl. Acad. Sci. U.S.A.* 105, 5099–5104).

Alzheimer disease is characterized by extracellular deposition of plaques of amyloid-β (Aβ)[2] peptides in the brain (1). These protein aggregates are composed of mature Aβ fibrils, which represent the end product of a long, complex, and not well understood fibrillation process (2, 3). The fibrillation pathway initiates with soluble unstructured monomeric Aβ peptides, which are converted into oligomers, protofibrils, and finally into mature fibrils (4–6). Recently, interest in the transient Aβ intermediate structures has been growing rapidly because these species are considered to represent the cytotoxic intermediates in Alzheimer disease (7). In addition to the well studied structure (8–12) and dynamics (13) of mature Aβ fibrils, a growing amount of data for oligomers (14–19) and protofibrils (20, 21) has become available. With regard to the secondary structure elements, these studies revealed that oligomers and protofibrils already exhibit the characteristic two β-strand sections connected by a short loop also present in mature Aβ fibrils. However, there are several significant differences between theses species. For instance, the first β-strand of Aβ oligomers and protofibrils is significantly shorter than that in mature Aβ fibrils and has to elongate during the conversion from protofibrils to mature fibrils (20). In addition, many questions about the tertiary structure, the fibrillation process, and the conversion from one intermediate to another are still unanswered.

Härd and co-workers have resolved the structure of Aβ(1–40) oligomers stabilized by an Affibody and also proposed a model for the arrangement of the two β-strands (14, 15, 22). In this model, these β-strands form intramolecular hydrogen bonds in the oligomeric state, in contrast to the known intermolecular hydrogen-bonded structure of mature Aβ fibrils (8, 11, 23). Such an arrangement is necessary to form the characteristic cross-β-structure, which is present in all amyloid protein fibrils. Therefore, the structural transition from Aβ oligomers into mature Aβ fibrils necessitates a 90° rotation of the β-strands upon maturation (see Fig. 1). The current model suggests that this switch from intra- to intermolecular hydrogen bonds occurs during the conversion from protofibrils to mature fibrils (14, 15). However, neither the tertiary structure nor the nature of the intra- *versus* intermolecular contacts in protofibrils has been investigated until now. So far, support for this model comes from the observation that double cysteine mutants of Aβ(1–40) and also Aβ(1–42), which are forced to retain the molecular structure of an oligomer by the cysteine bond, can form only protofibrils but not mature fibrils (14, 22). In addition, it was shown by IR spectroscopy that, in oligomers and protofibrils, the β-sheets are antiparallel (18, 24), whereas mature Aβ fibrils exhibit parallel β-sheets as shown by solid-state NMR (25).

To obtain more structural data, we used ^{13}C solid-state NMR to investigate the contact between Glu-22 and Ile-31 of Aβ(1–40) protofibrils, which are by stabilized by the B10AP antibody as reported previously (24). Glu-22 and Ile-31 and, in particular, the side chains of these residues should become very close in space in the oligomeric structure as illustrated in Fig. 1. From the Protein Data Bank coordinates (15), one can calculate a distance of 5.3 Å between the α-carbons of Glu-22 and Ile-31;

* This work was supported by the Deutsche Forschungsgemeinschaft (Grants Transregio-SFB 102 and A6 and a personal grant to I. M.).
[S] This article contains supplemental Figs. S1–S4.
[1] To whom correspondence should be addressed: Inst. of Medical Physics and Biophysics, University of Leipzig, Härtelstr. 16–18, D-04107 Leipzig, Germany. Tel.: 49-341-97-15701; Fax: 49-341-97-15709; E-mail: daniel.huster@medizin.uni-leipzig.de.
[2] The abbreviation used is: Aβ, amyloid-β.

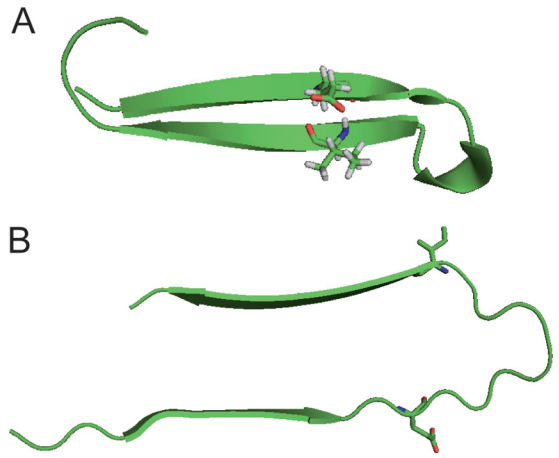

FIGURE 1. **Molecular structures of Aβ(1–40) oligomers (*A*; Protein Data Bank code 2OTK (15)) and mature Aβ fibrils (*B*; Ref. 11 and I. Bertini, personal communication).** Glu-22 and Ile-31 are shown in their molecular structure. For Aβ protofibrils, no molecular structure is available so far.

the side chain carbons show similar close proximities. In contrast, in mature Aβ fibrils (11), these residues point into different directions out of the cross-β-core of the fibrils, yielding a distance of 12.4 Å between the α-carbons of Glu-22 and Ile-31 and up to ~18 Å between the side chain carbons. This is illustrated in Fig. 1 using the Protein Data Bank coordinates of these two structures. For protofibrils, no molecular structure with atomic resolution is available so far, but solid-state NMR work revealed that the secondary structure elements of protofibrils are more closely related to oligomers than to mature Aβ fibrils (20). Therefore, solid-state NMR measurements should reveal the arrangement of the two β-sheets in protofibrils and give insights in their tertiary fold.

EXPERIMENTAL PROCEDURES

The Aβ(1–40) peptides were produced by standard solid-phase synthesis according to the Fmoc (*N*-(9-fluorenyl)methoxycarbonyl) protocol using fully $^{13}C/^{15}N$-labeled Ser-8, Glu-22, and Ile-31. B10AP-stabilized protofibrils were prepared in 1-ml samples (50 mM Hepes (pH 7.4) and 50 mM NaCl) containing 4 mg/ml labeled Aβ(1–40) and B10AP at a 10:1 molar ratio. The samples were incubated for 3 days (37 °C).

For mature Aβ(1–40) fibrils, the labeled peptide was solubilized in 50 mM sodium borate buffer (pH 9) at a concentration of 6 mg/ml. The sample was seeded and incubated at 37 °C for 1 week. Seeds consisted of Aβ(1–40) mature fibrils previously grown and seeded under the same conditions (second generation) and were sonicated for 10 min before addition to the sample. It has been shown that, also under these conditions, the structural properties of the mature fibrils agreed well with fibrils grown at pH 7.4 in phosphate buffer (13).

In both cases, the peptide aggregates were recovered by ultracentrifugation at 100,000 rpm for 2 h at 4 °C (TLA-120.2 rotor, Beckman Optima TLX centrifuge). The pellet was lyophilized, rehydrated with 50 weight % H_2O, and homogenized by freezing the sample in liquid nitrogen and thawing it at 37 °C. The morphology of the samples was checked by transmission electron microscopy (supplemental Fig. S1).

The ^{13}C cross-polarization magic angle spinning NMR spectra were obtained using a Bruker AVANCE 750 spectrometer (Bruker BioSpin GmbH, Rheinstetten, Germany) operating at resonance frequencies of 749.7 MHz for ^1H and 188.5 MHz for ^{13}C. A 4-mm double-resonance magic angle spinning probe was used. The length of the cross-polarization contact time was 700 μs, and the 90° pulse was 5 μs for ^{13}C and 4 μs for ^1H. For heteronuclear two-pulse phase modulation decoupling, a ^1H radiofrequency field of 65 kHz was applied. ^{13}C chemical shifts were referenced externally relative to TMS. The peak assignment was taken from the literature (13, 20). The two-dimensional ^{13}C-^{13}C proton-driven spin exchange spectra were acquired with a mixing time of 600 ms and covariance-processed (26). A total of 64 complex data points were acquired in the indirect dimension at a spectral width of 190 ppm. For the protofibrils, 640 transients per increment were acquired, whereas 2096 scans were acquired for two-dimensional spectra of the mature Aβ fibrils at 58 t_1 increments.

To measure ^{13}C-^1H dipolar couplings, constant time DIPSHIFT experiments with FSLG (frequency-switched Lee-Goldburg) (27) or MREV-8 (28) for homonuclear decoupling (80-kHz decoupling field) were performed. The order parameter was derived by dividing the determined coupling by the known rigid limits (29, 30). All NMR experiments were carried out at a temperature of 30 °C and a magic angle spinning frequency of 7 or 5 kHz (DIPSHIFT or MREV-8).

RESULTS

Fig. 2 shows characteristic ^{13}C-^{13}C proton-driven spin diffusion correlation spectra of Aβ(1–40) protofibrils (*panel A*) and mature Aβ fibrils (*panel B*) both with uniformly $^{13}C/^{15}N$-labeled Ser-8, Glu-22, and Ile-31. The spectra show all of the trivial intraresidue correlations within the labeled amino acids. As a long mixing time of 600 ms was used, also interresidue correlations can be observed. All magnetization exchange, which gives rise to a cross-peak in the proton-driven spin diffusion spectra, is caused by dipolar interactions with a distance dependence of r^{-6} (31).

In addition, the ^{13}C-^{13}C correlation spectra of Aβ protofibrils clearly show cross-peaks between Glu-22 and Ile-31, especially between the Cα and Cβ signals of Glu-22 at 52.6 and 32.6 ppm and between the Cδ and Cε signals of Ile-31 at 16.1 and 12.5 ppm. This means that, in Aβ protofibrils, Ile-31 and Glu-22 are in close proximity (<6–7 Å), which is observable by ^{13}C-^{13}C correlation spectroscopy (32). The cross-peaks between the other carbons of these two amino acids (including the cross-peak Glu-22 Cα–Ile-31 Cα) are weaker and only sparsely above the noise level, even when using covariance NMR processing, which is known to enhance small cross-peaks (33). For comparison, the standard Fourier transform-processed two-dimensional NMR spectrum is shown in supplemental Fig. S2.

For comparison, we conducted the same experiment using mature Aβ fibrils grown from Aβ(1–40) peptides using the same amino acid labeling procedure. In the NMR spectrum of this sample (Fig. 2*B* and supplemental Fig. S2*B*), no cross-peaks between Glu-22 and Ile-31 are visible, as expected from the molecular structure of mature fibrils (Fig. 1*B*). Please note that there are some differences in the chemical shift values between

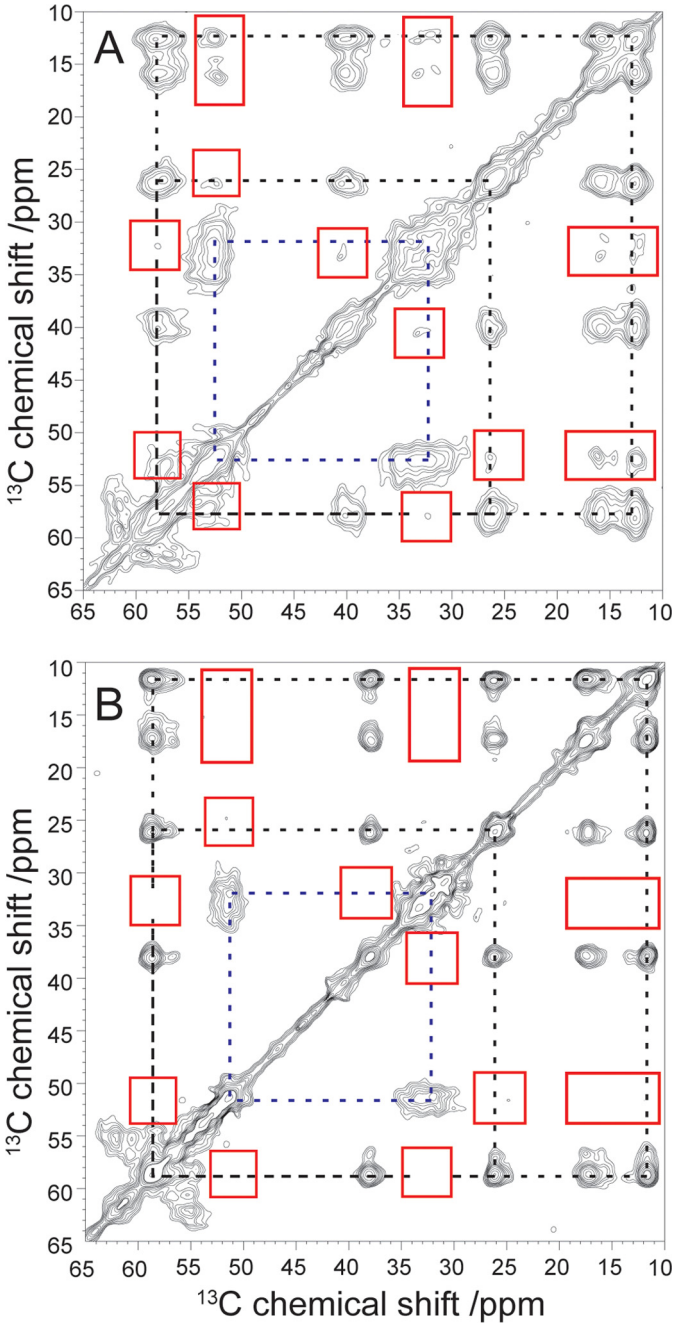

FIGURE 2. **Aliphatic region of the covariance-processed ^{13}C-^{13}C correlation spectra (by proton-driven spin diffusion with a mixing time of 600 ms) for B10AP-stabilized Aβ protofibrils (*A*) and mature Aβ fibrils (*B*).** The major correlations inside one and the same amino acid for Glu-22 (*dashed blue lines*) and Ile-31 (*dashed black lines*) are highlighted. Interresidue cross-peaks between Glu-22 and Ile-31 in *A* and the lack of these cross-peaks in *B* are marked with *red boxes*.

Aβ protofibrils and mature Aβ fibrils for these amino acids as reported previously (13, 20).

To confirm that the differences in the NMR spectra are not just the result of the choice of contour levels in the two-dimensional plots, we also extracted slices from the two-dimensional spectra, which are shown in Fig. 3 (see also supplemental Fig. S3 for the standard Fourier transform-processed spectra). Again, the cross-peaks from Glu-22 to the side chain of Ile-31 are only observable for the Aβ protofibrils but not for the mature Aβ fibrils.

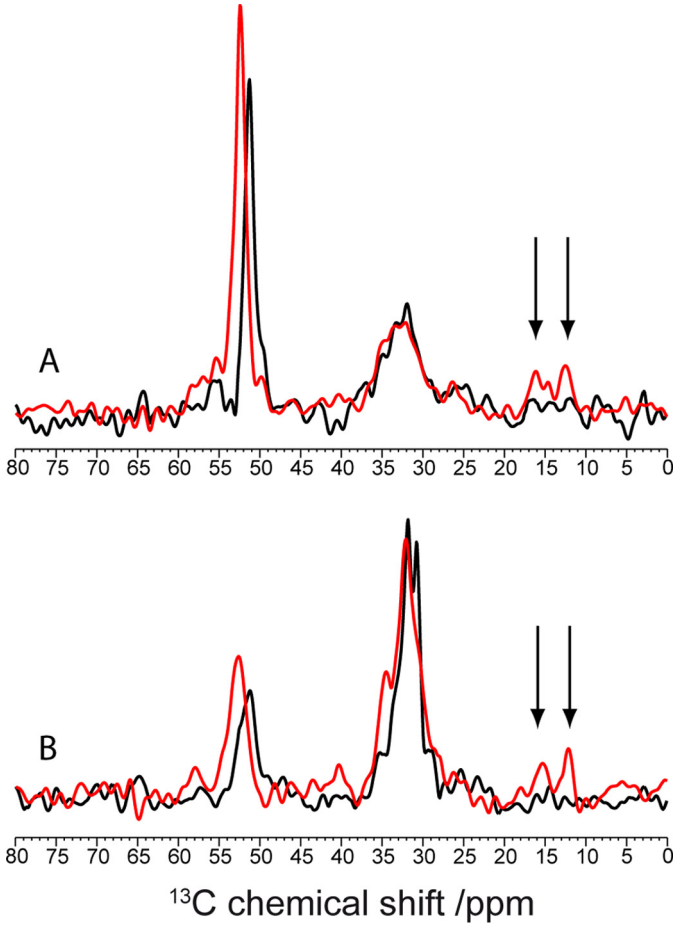

FIGURE 3. **Slices through the Cα (*A*) and Cβ (*B*) peaks of Glu-22 for B10AP-stabilized Aβ protofibrils (*red*) and mature Aβ fibrils (*black*) of the covariance-processed proton-driven spin diffusion spectra.** Interresidue cross-peaks between Glu-22 and Ile-31 are highlighted by the *arrows*.

The structural differences in Aβ protofibrils and mature fibrils are also reflected in the molecular dynamics of the residues investigated. As shown in Fig. 4, the order parameters of the amino acid side chains determined from motionally averaged dipolar couplings show a clear tendency to be lower in mature Aβ fibrils than in Aβ protofibrils. If one assumes a similar structural arrangement of the β-sheets in Aβ oligomers (Fig. 1) and in protofibrils, the interaction of the side chains of Glu-22 and Ile-31 leads to a motional restriction and therefore the higher order parameters in protofibrils. The decreased order parameters of these side chains in mature Aβ fibrils are caused by the additional degrees of motional freedom the side chains can undergo when they are pointing out of the cross-β-core of the fibrils (Fig. 1). It should be noted that binding of the B10 antibody has no significant influence on the order parameters of Glu-22 and Ile-31 (13, 20).

DISCUSSION

We conclude that Glu-22 and Ile-31 are in close proximity in Aβ protofibrils but are significantly more distant in mature Aβ fibrils (as suggested by the structural model of both species sketched in Fig. 1*B*). This means that the Aβ protofibrils share some similarity in tertiary structure with Aβ oligomers, a finding that was already suggested from the analysis of secondary

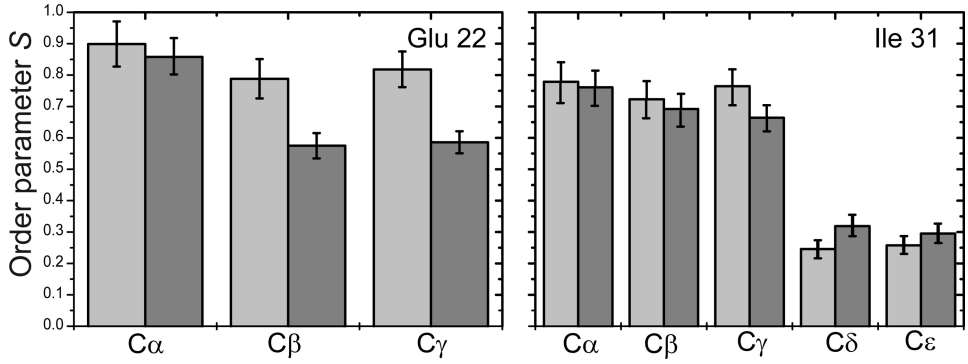

FIGURE 4. **C-H order parameters for Glu-22 and Ile-31 in B10AP-stabilized Aβ protofibrils (*light gray bars*) and mature Aβ fibrils (*dark gray bars*).**

chemical shifts (20). Further support for this conclusion comes from a previous experimental finding that Phe-19 and Leu-34 are in close proximity in Aβ protofibrils (20) as well as in oligomers (16), where the distance between the Phe ring and Leu δ-carbons is 3.9 Å. However, contacts between the side chains of these residues have also been observed in mature Aβ fibrils (distance of ~7 Å) (10, 34), rendering this pair of residues less indicative of a tertiary structural conversion from protofibrils to mature Aβ fibrils.

Our findings suggest that there has to be a rearrangement of the two β-strands of Aβ protofibrils during the conversion to mature Aβ fibrils. Of course, we can only speculate about the nature of the hydrogen bonds in protofibrils, but because the close proximity between Glu-22 and Ile-31 is already known from Aβ oligomers (15), one can assume that the β-strands in Aβ protofibrils may also form intramolecular hydrogen bonds. This can be comprehended by a closer structural relationship between Aβ oligomers and protofibrils compared with protofibrils and mature fibrils as was suggested on the basis of ^{13}C chemical shift data (20), the capability of the cysteine mutant to form protofibrils (14, 22), and the known IR data, which indicate antiparallel β-sheets in protofibrils (18, 24). Therefore, it seems possible that the rearrangement of the intramolecular hydrogen bonds to the intermolecular hydrogen bonds takes place in the final structural transition from Aβ protofibrils to mature fibrils. Consequently, our solid-state NMR data would support the model for the aggregation mechanism of Aβ fibrils suggested by Härd and co-workers (15).

Acknowledgments—We thank the Deutsche Forschungsgemeinschaft and the Institute of Experimental Physics of the University of Leipzig for measuring time on the AVANCE 750 spectrometer.

REFERENCES

1. Holtzman, D. M., Morris, J. C., and Goate, A. M. (2011) Alzheimer disease: the challenge of the second century. *Sci. Transl. Med.* **3,** 77sr1
2. Finder, V. H., and Glockshuber, R. (2007) Amyloid-βaggregation. *Neurodegener. Dis.* **4,** 13–27
3. Morgado, I., and Fändrich, M. (2011) Assembly of Alzheimer Aβ peptide into nanostructured amyloid fibrils. *Curr. Opin. Colloid Interface Sci.* **16,** 508–514
4. Goldsbury, C. S., Wirtz, S., Müller, S. A., Sunderji, S., Wicki, P., Aebi, U., and Frey, P. (2000) Studies on the *in vitro* assembly of Aβ(1–40): implications for the search for Aβ fibril formation inhibitors. *J. Struct. Biol.* **130,** 217–231
5. Harper, J. D., Wong, S. S., Lieber, C. M., and Lansbury, P. T. (1997) Observation of metastable Aβ amyloid protofibrils by atomic force microscopy. *Chem. Biol.* **4,** 119–125
6. Dasilva, K. A., Shaw, J. E., and McLaurin, J. (2010) Amyloid-β fibrillogenesis: structural insight and therapeutic intervention. *Exp. Neurol.* **223,** 311–321
7. Lashuel, H. A., and Lansbury, P. T., Jr. (2006) Are amyloid diseases caused by protein aggregates that mimic bacterial pore-forming toxins? *Q. Rev. Biophys.* **39,** 167–201
8. Petkova, A. T., Ishii, Y., Balbach, J. J., Antzutkin, O. N., Leapman, R. D., Delaglio, F., and Tycko, R. (2002) A structural model for Alzheimer β-amyloid fibrils based on experimental constraints from solid-state NMR. *Proc. Natl. Acad. Sci. U.S.A.* **99,** 16742–16747
9. Paravastu, A. K., Petkova, A. T., and Tycko, R. (2006) Polymorphic fibril formation by residues 10–40 of the Alzheimer β-amyloid peptide. *Biophys. J.* **90,** 4618–4629
10. Paravastu, A. K., Leapman, R. D., Yau, W. M., and Tycko, R. (2008) Molecular structural basis for polymorphism in Alzheimer β-amyloid fibrils. *Proc. Natl. Acad. Sci. U.S.A.* **105,** 18349–18354
11. Bertini, I., Gonnelli, L., Luchinat, C., Mao, J., and Nesi, A. (2011) A new structural model of Aβ40 fibrils. *J. Am. Chem. Soc.* **133,** 16013–16022
12. Lührs, T., Ritter, C., Adrian, M., Riek-Loher, D., Bohrmann, B., Döbeli, H., Schubert, D., and Riek, R. (2005) 3D structure of Alzheimer amyloid-β(1–42) fibrils. *Proc. Natl. Acad. Sci. U.S.A.* **102,** 17342–17347
13. Scheidt, H. A., Morgado, I., Rothemund, S., and Huster, D. (2012) Dynamics of amyloid-β fibrils revealed by solid-state NMR. *J. Biol. Chem.* **287,** 2017–2021
14. Sandberg, A., Luheshi, L. M., Söllvander, S., Pereira de Barros, T., Macao, B., Knowles, T. P., Biverstål, H., Lendel, C., Ekholm-Petterson, F., Dubnovitsky, A., Lannfelt, L., Dobson, C. M., and Härd, T. (2010) Stabilization of neurotoxic Alzheimer amyloid-β oligomers by protein engineering. *Proc. Natl. Acad. Sci. U.S.A.* **107,** 15595–15600
15. Hoyer, W., Grönwall, C., Jonsson, A., Ståhl, S., and Härd, T. (2008) Stabilization of a β-hairpin in monomeric Alzheimer amyloid-β peptide inhibits amyloid formation. *Proc. Natl. Acad. Sci. U.S.A.* **105,** 5099–5104
16. Ahmed, M., Davis, J., Aucoin, D., Sato, T., Ahuja, S., Aimoto, S., Elliott, J. I., Van Nostrand, W. E., and Smith, S. O. (2010) Structural conversion of neurotoxic amyloid-β(1–42) oligomers to fibrils. *Nat. Struct. Mol. Biol.* **17,** 561–567
17. Chimon, S., Shaibat, M. A., Jones, C. R., Calero, D. C., Aizezi, B., and Ishii, Y. (2007) Evidence of fibril-like β-sheet structures in a neurotoxic amyloid intermediate of Alzheimer β-amyloid. *Nat. Struct. Mol. Biol.* **14,** 1157–1164
18. Cerf, E., Sarroukh, R., Tamamizu-Kato, S., Breydo, L., Derclaye, S., Dufrêne, Y. F., Narayanaswami, V., Goormaghtigh, E., Ruysschaert, J. M., and Raussens, V. (2009) Antiparallel β-sheet: a signature structure of the oligomeric amyloid-β peptide. *Biochem. J.* **421,** 415–423
19. Haupt, C., Leppert, J., Rönicke, R., Meinhardt, J., Yadav, J. K., Ramachandran, R., Ohlenschläger, O., Reymann, K. G., Görlach, M., and Fändrich, M. (2012) Structural basis of β-amyloid-dependent synaptic dysfunctions. *Angew. Chem. Int. Ed. Engl.* **51,** 1576–1579

20. Scheidt, H. A., Morgado, I., Rothemund, S., Huster, D., and Fändrich, M. (2011) Solid-state NMR spectroscopic investigation of Aβ protofibrils: implication of a β-sheet remodeling upon maturation into terminal amyloid fibrils. *Angew. Chem. Int. Ed. Engl.* **50,** 2837–2840
21. Fawzi, N. L., Ying, J., Ghirlando, R., Torchia, D. A., and Clore, G. M. (2011) Atomic resolution dynamics on the surface of amyloid-β protofibrils probed by solution NMR. *Nature* **480,** 268–272
22. Härd, T. (2011) Protein engineering to stabilize soluble amyloid-β protein aggregates for structural and functional studies. *FEBS J.* **278,** 3884–3892
23. Paravastu, A. K., Qahwash, I., Leapman, R. D., Meredith, S. C., and Tycko, R. (2009) Seeded growth of β-amyloid fibrils from Alzheimer brain-derived fibrils produces a distinct fibril structure. *Proc. Natl. Acad. Sci. U.S.A.* **106,** 7443–7448
24. Habicht, G., Haupt, C., Friedrich, R. P., Hortschansky, P., Sachse, C., Meinhardt, J., Wieligmann, K., Gellermann, G. P., Brodhun, M., Götz, J., Halbhuber, K. J., Röcken, C., Horn, U., and Fändrich, M. (2007) Directed selection of a conformational antibody domain that prevents mature amyloid fibril formation by stabilizing Aβ protofibrils. *Proc. Natl. Acad. Sci. U.S.A.* **104,** 19232–19237
25. Antzutkin, O. N. (2004) Amyloidosis of Alzheimer Aβ peptides: solid-state nuclear magnetic resonance, electron paramagnetic resonance, transmission electron microscopy, scanning transmission electron microscopy, and atomic force microscopy studies. *Magn. Reson. Chem.* **42,** 231–246
26. Zhang, F., and Brüschweiler, R. (2004) Indirect covariance NMR spectroscopy. *J. Am. Chem. Soc.* **126,** 13180–13181
27. Munowitz, M. G., Griffin, R. G., Bodenhausen, G., and Huang, T. H. (1981) Two-dimensional rotational spin-echo nuclear magnetic resonance in solids: correlation of chemical shift and dipolar interactions. *J. Am. Chem. Soc.* **103,** 2529–2533
28. Rhim, W. K., Elleman, D. D., and Vaughan, R. W. (1973) Enhanced resolution for solid-state NMR. *J. Chem. Phys.* **58,** 1772–1773
29. Barre, P., Zschornig, O., Arnold, K., and Huster, D. (2003) Structural and dynamical changes of the bindin B18 peptide upon binding to lipid membranes. A solid-state NMR study. *Biochemistry* **42,** 8377–8386
30. Huster, D., Xiao, L., and Hong, M. (2001) Solid-state NMR investigation of the dynamics of the soluble and membrane-bound colicin Ia channel-forming domain. *Biochemistry* **40,** 7662–7674
31. Schmidt-Rohr, K., and Spiess, H. W. (1994) *Multidimensional Solid-State NMR and Polymers*, pp. 95–98, Academic Press, London
32. Huster, D. (2005) Investigations of the structure and dynamics of membrane-associated peptides by magic angle spinning NMR. *Prog. Nucl. Magn. Reson. Spectrosc.* **46,** 79–107
33. Masuda, Y., Fukuchi, M., Yatagawa, T., Tada, M., Takeda, K., Irie, K., Akagi, K., Monobe, Y., Imazawa, T., and Takegoshi, K. (2011) Solid-state NMR analysis of interaction sites of curcumin and 42-residue amyloid-β protein fibrils. *Bioorg. Med. Chem.* **19,** 5967–5974
34. Tycko, R. (2006) Molecular structure of amyloid fibrils: insights from solid-state NMR. *Q. Rev. Biophys.* **39,** 1–55